

DEVELOPMENT OF CAPACITIVE EXTENSOMETER WITH VERSATILITY SUPERIOR TO THE RESISTIVE EXTENSOMETER

^{1,2}Josivaldo G. Silva, ¹Isabella F. Rondon, ¹Andrés B. Cheung and ¹Felipe S. Matos

¹Faculty of Engineering, Architecture and Geography, Federal University of Mato Grosso of Sul, State of Mato Grosso of Sul, BRA

²Post-Graduation Health Center-West, School of Medicine - FAMED, Federal University of Mato Grosso do Sul, State of Mato Grosso do Sul, BRA

ARTICLE INFO

Article History:

Received 15th April, 2018
Received in revised form
17th May, 2018
Accepted 20th June, 2018
Published online 30th July, 2018

Key Words:

Capacitive Extensometer, Electrodes,
Stainless Steel, Versatility.

ABSTRACT

The objective of this work was to develop a capacitive extensometer containing four identical capacitive sensors that went connected in the two branches of a Wheatstone Bridge. The electrodes of the capacitive sensors were made of stainless steel to avoid corrosion with the humidity that would impair the response of the extensometer. Each sensor has an immobile electrode measuring 8.0 mm in length, 5.0 mm in width and 0.1 mm in thickness by being bonded onto an insulation holder developed with PA 66 polyamide polymer. There are two identical mobile electrodes measuring 40.0 mm in length, 5.0 mm in width and 0.1 mm in thickness, which are common to four capacitive sensors. These electrodes were bonded to the opposite faces of the same polyethylene polymer that moves when the extensometer undergoes stretching or shortening. It was verified that the extensometer can be stimulated with sinusoidal voltage higher than 10 Vac and frequency higher than 59 Hz, its response was linear with hysteresis of 3.0%, response time of 8.0 ms, resolution of 0.09 N. The new extensometer has higher sensitivity, 1.0 V while resistive extensometer presented 0.20 V. This capacitive extensometer has the potential to do measure several different physical magnitudes.

Copyright © 2018, Josivaldo G. Silva et al. This is an open access article distributed under the Creative Commons Attribution License, which permits unrestricted use, distribution, and reproduction in any medium, provided the original work is properly cited.

Citation: Josivaldo G. Silva, Isabella F. Rondon, Andrés B. Cheung and Felipe S. Matos, 2018. "Development of capacitive extensometer with versatility superior to the resistive extensometer", *International Journal of Development Research*, 8, (06), 21736-21740.

INTRODUCTION

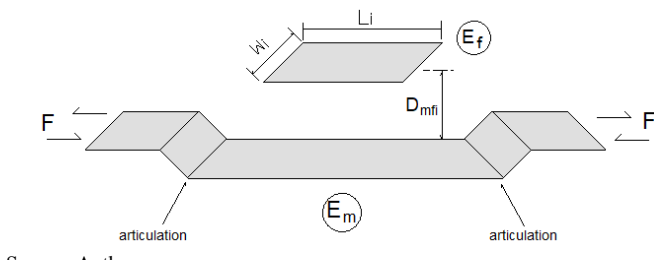
The extensometers are devices that respond electrically to the deformation suffered that is due to the accomplishment of mechanical effort in the mechanical structure where they are bonded. In the case of the electrical methodology in general, the electric extensometer is used in which the deformation that occurs in the mechanical material causes variations in the capacitance, inductance or electrical resistance (Areny, 1991). Due to the importance of extensometers, scientists and companies have developed several important devices for their applications. Relevant searches showing different applications are presented in the next few paragraphs (Cobbold, 1974).

*Corresponding author: Josivaldo G. Silva

¹Faculty of Engineering, Architecture and Geography, Federal University of Mato Grosso of Sul, State of Mato Grosso of Sul, BRA

²Post-Graduation Health Center-West, School of Medicine - FAMED, Federal University of Mato Grosso do Sul, State of Mato Grosso do Sul, BRA

Zeiser, Fellner and Wilde (2014) developed a novel capacitive strain gage with interdigital electrodes, which was processed on Polyimide and Liquid Crystal Polymer (LCP) foil substrates. The metallization is deposited and patterned using thin-film technology with structure sizes down to 15 μm . The characterization of the strain sensors after fabrication revealed the gage factor (GF) as well as the cross sensitivities on temperatures up to 100 $^{\circ}\text{C}$ and relative humidity up to 100%. The GF of a sensor with an electrode width of 45 μm and a clearance of 15 μm was -1.38 at a capacitance of 48 pF. The GF of a sensor half-bridge consisting of two orthogonal capacitors was 2.3. Zens et al. (2015) developed proposed polydimethylsiloxane strain (PS) as a non-invasive, highly accurate and easy to use measurement method to quantify the anterolateral and rotational loops of the knee joint during active and passive movement. In this work a prototype was developed and measurements were made using a knee test equipment, which was designed for this purpose.



Source: Author

Figure 1. C_S structure

The sensitivity of the sensor was determined to be 2.038. Optimal positions of the sensors to capture the bone-to-bone displacement as the projected displacement on the skin were identified. Kim SR, Kim JH and Park JW (2017) developed capacitive sensor (C_S) or to measure deformation (ε) made with transparent and extensible thin film based on Ag nanoparticles (*AgNWs*). The *AgNWs* employed a capillary force lithography (*CFL*) method and were incorporated into the surface of the polydimethylsiloxane substrate. The sensitivity of the sensor was controlled by the standardization of *AgNWs* in electrodes using interdigitated form. This interdigitated capacitive deformation sensor (*ICSS*) presented a *GF* of -1.57 at 30% considered higher than the sensitivity of capacitive deformation sensors of traditional parallel plates. Because of the interdigitated electrode pattern, the *GF* was increased to -2.0. The *ICSS* did not show hysteresis for values of ε up to 15% and presented stable performance during the repeated elongation test with ε values of 10% for 1000 cycles. The *ICSS* was used to detect muscular movements of the fingers and the pulses of the human body.

This paper presents a new capacitive extensometer (E_c), developed to be used in load cells to determine mechanical magnitudes such as force (F), vibration, deformation ε and pressure in structural systems. The result was not affected by the ambient temperature variation $\Delta(t)$, even by dielectric permittivity variation $\Delta(\xi)$. The device is simple to build, rugged, has affordable cost and great versatility.

Theoretical foundations: The C_S structure was idealized because the capacitance variation (Δc) due spacing variation (ΔD_{mf}) between the fixed electrode (E_f) and the mobile electrode (E_m) being than ΔD_{mf} arises in the occurrence of the force F . Figure 1 shows the fundamental structure of the C_S .

Applying the Hook's Law is obtained the equation (1) shows the relationship between F , ε_L , E and A_s of the metal rod (B).

$$F = \varepsilon_L E A_s \quad (1)$$

Being E : Young's Module; ε_L : longitudinal deformation on the B and A_s : metal rod cross-sectional area. The C_S or has smooth and parallel electrodes whose initial capacitance (C_i) shown in equation (2) does not suffer the effect of the temperature variation and also does not suffer the variation of the dielectric permittivity.

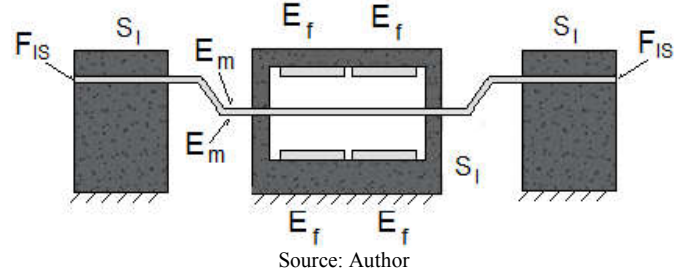
$$C_i = \frac{\xi_i L_i W_i}{D_{mfi}} \quad (2)$$

Being ξ_i : initial dielectric permittivity; L_i : initial length of E_f and W_i : initial width of E_f . In equation (3), therefore, ε_L is reformulated considering application of F normal of traction, F normal of compression or F of shear in the B as shown below.

$$\varepsilon_L = \frac{(c_f - c_i)}{c_i} \quad (3)$$

Being c_f : final capacitance.

Figure 2 shows the side view of the E_c developed containing the four capacitive sensors. This E_c was bonded onto a B in which it can be applied F . The E_f were bonded to the acrylic insulation support (S_i) while E_m were separated from each other by a flexible insulation film (F_{is}).



Source: Author

Figure 2. Capacitive Extensometer

If F of traction occurs on B , the vertical displacement of E_m will be upwards, reducing D_{mf} and therefore the Δc will be positive. Equation (4) shows the relationship between the Δc and F .

$$F = \frac{\Delta c}{c} E A_s \quad (4)$$

(4)

Doing $k_1 = \frac{\Delta c}{c} E$, will get the equation (5).

$$F = k_1 \Delta c \quad (5)$$

If F of compression occurs on the B , the vertical displacement of E_m will be down, increasing D_{mf} and, therefore the Δc , will be negative. Equation (6) shows the relationship between Δc and F .

$$F = -k_1 \Delta c \quad (6)$$

Besides that, figure (2) shows three effects that occur being that in the first caused by F the capacitive sensors S_{1C} and S_{2C} generate identical responses while the capacitive sensors S_{3C} and S_{4C} also generate identical responses. The second effects to consider is the of the temperature variation Δt in L_i , W_i and ξ_i that causes $\Delta c(t)$ equal in the four C_S . The third effect to consider that causes Δc of the capacitive sensors is the variation of the external environment that causes the variation in dielectric permittivity ($\Delta \xi$). However, since the four C_S are identical Δc (ξ) is the same in all. Thus, the responses of S_{1C} and S_{2C} if F of traction is shows in the equation (7).

$$\Delta c(t, \xi, F) = \Delta c(t) + \Delta c(\xi) + \Delta c(F) \quad (7)$$

While, the responses of S_{3C} and S_{4C} is shows in the equation (8).

$$\Delta c(t, \xi, F) = \Delta c(t) + \Delta c(\xi) - \Delta c(F) \quad (8)$$

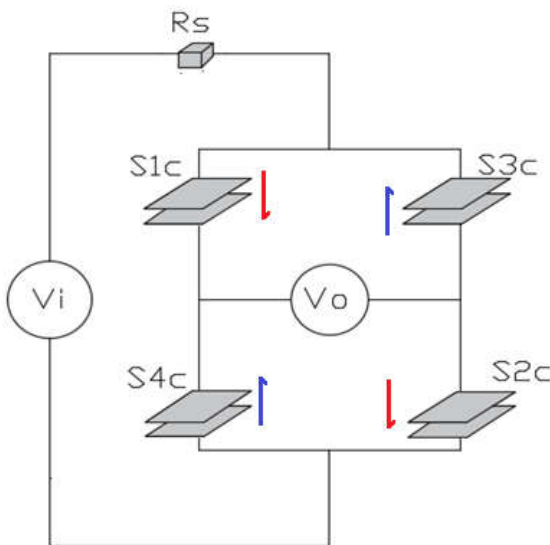
Thus, the responses of S_{1C} and S_{2C} if F of compression is shows in the equation (9).

$$\Delta c(t, \xi, F) = \Delta c(t) + \Delta c(\xi) - \Delta c(F) \quad (9)$$

While, the responses of S_{3c} and S_{4c} is shown in the equation (10).

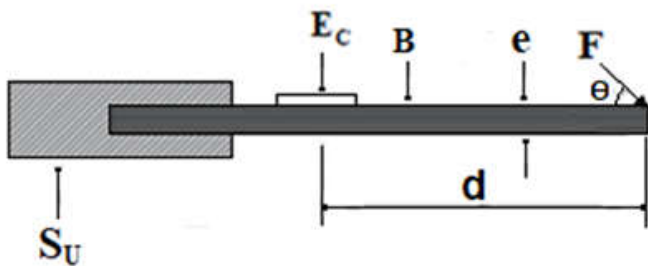
$$\Delta c(t, \xi, F) = \Delta c(t) + \Delta c(\xi) + \Delta c(F) \tag{10}$$

Figure 3 shows the Wheatstone Bridge circuit containing the capacitive sensors. The E_c was implemented, aiming to obtain sensitivity and to eliminate in the response V_0 the undesirable effects of $\Delta c(t)$ and $\Delta c(\xi)$. The resistance (R_s) is necessary to avoid short circuit and the positions occupied by the capacitive sensors are fundamental. Figure 4 shows the mechanical structure of the load cell. Where the E_c was bonded and B underwent deformation due to the application of F . Being S_u : support; e : thickness; d : distance of F to E_c .



Source: Author.

Figure 3. Wheatstone Bridge



Source: Author

Figure 4. Load cell structure

Finally, the capacitive extensometer response is defined by equation (11).

$$V_0 = \varepsilon_L \frac{(1 + \nu)V_i}{2} \tag{11}$$

Being ν : Poisson's Coefficient.

Relating ε_L of equation (11) with equation (1) is obtained equation (12).

$$V_0 = F \frac{V_i(1 + \nu)}{2A_S E} \tag{12}$$

Equation (13) presents a constant k_2 .

$$k_2 = \frac{V_i(1 + \nu)}{2A_S E} \tag{13}$$

Equation (14) corresponds to the introduction of k_2 in the equation (12).

$$V_0 = F k_2 \tag{14}$$

METHODOLOGY AND MATERIALS

The current research was developed in the laboratory of Sensors, Electronic Instrumentation and Metrology of Federal University of Mato Grosso do Sul – UFMS. The project consisted in the implementation of an E_c formed by one capacitive Wheatstone Bridge with four identical capacitive sensors. The design of the Wheatstone Bridge with C_S is shown in figure 3. A resistor, made of metallic film with 150Ω , was connected in series with the circuit in Wheatstone Bridge, aiming to avoid short circuit in S_{1c} , S_{2c} , S_{3c} and S_{4c} . Each sensor has an immobile electrode measuring 8.0 mm in length, 5.0 mm in width and 0.1 mm in thickness by being bonded onto an insulation holder developed with PA 66 polyamide polymer. D_{mfi} was 0.5 mm. The adhesive used to fix E_f , E_m and E_c was a generic use cyanoacrylate, and the S_f was developed in acrylic. The advantage of used methodology is to compare the electric potential difference in the two branches of the bridge, to eliminate the undesirable temperature variation effect and the permittivity dielectric. Figure 3 shows the E_c formed by one Wheatstone Bridge using one sinusoidal voltage source to guarantee the charging (V_i), electric current and necessary frequency. Besides, the same V_i will allow to compensate the $\Delta c(t)$ and $\Delta c(\xi)$. V_i applied by the source was about 10 Vac with frequency of 20 kHz. The model of the voltage source is DEGEM PU 2222 (Minipa). Figure 4 shows E_c attached to B thus constituting a type of load cell in which F was applied at the extremity. The signal conditioning circuit was developed to process the electrical potential difference between the adjacent branches of the E_c . The operational amplifiers (OA) LF356 (National Semiconductor), used in the signal conditioning circuit, were powered by the constant voltage source MPC 3006D (Minipa) which provided +12 V and -12 V.

Signal Conditioning Circuit: An electronic signal conditioning circuit was implemented to treat the response of E_c . The circuit was formed by five blocks (B_1 , B_2 , B_3 and B_4) containing OA. The block B_1 , made in Wein Bridge, generates a 10 Vac voltage with a frequency of 20 kHz, to stimulate E_c . V_0 was submitted to the inverting amplifier (B_2) to perform other amplification with gain of $3 \cdot 10^3$ was connected to the bandpass filter (B_3) to exclude electromagnetic noise whose frequencies were less than 19 kHz and 21 kHz. B_3 is of fourth order with has *MFB* structure to operate with bandwidth of 2 kHz and gain of 10 and your response was connected to the peak detector (B_4) to obtain the amplitude of the E_c response, measured by a digital two-channel oscilloscope model 54603 B (HP).

Answer Comparison: The comparison between E_c and the conventional resistive extensometer (E_R), developed with four resistive sensors, each with a resistance of 350Ω . Both extensometers were connected to the same voltage and subjected to the same experimental conditions, using the same signal conditioning circuit and the same mechanical structure, shown in figure 4.

Table 1. Response adding mass

| MassAdded(g) | Response (V) | | | | | | A | S. D |
|--------------|--------------|------|------|------|------|------|------|------|
| | R1 | R2 | R3 | R4 | R5 | R6 | | |
| 00 | 0.00 | 0.00 | 0.00 | 0.00 | 0.00 | 0.00 | 0.00 | 0.00 |
| 50 | 0.23 | 0.21 | 0.22 | 0.23 | 0.22 | 0.23 | 0.23 | 0.01 |
| 100 | 0.50 | 0.48 | 0.49 | 0.50 | 0.49 | 0.49 | 0.49 | 0,01 |
| 150 | 0.70 | 0.69 | 0.68 | 0.70 | 0.69 | 0.69 | 0.69 | 0,01 |
| 200 | 0.93 | 0.90 | 0.91 | 0.93 | 0.93 | 0.92 | 0.92 | 0,01 |
| 250 | 1.17 | 1.15 | 1.16 | 1.17 | 1.17 | 1.17 | 1.17 | 0.01 |

Source: Author

Table 2. Response removing mass

| MassDecrease(g) | Response (V) | | | | | | A | S. D |
|-----------------|--------------|------|------|------|------|------|------|------|
| | R1 | R2 | R3 | R4 | R5 | R6 | | |
| 250 | 1.17 | 1.15 | 1.16 | 1.17 | 1.17 | 1.17 | 1.17 | 0.01 |
| 200 | 0.92 | 0.92 | 0.91 | 0.93 | 0.93 | 0.92 | 0.92 | 0.01 |
| 150 | 0.69 | 0.67 | 0.67 | 0.68 | 0.67 | 0.68 | 0.68 | 0.01 |
| 100 | 0.48 | 0.49 | 0.49 | 0.49 | 0.49 | 0.48 | 0.49 | 0.01 |
| 50 | 0.23 | 0.23 | 0.21 | 0.23 | 0.23 | 0.23 | 0.23 | 0.01 |
| 00 | 0.00 | 0.00 | 0.00 | 0.00 | 0.00 | 0.00 | 0.00 | 0.00 |

Source: Author.

To apply F , a stainless steel rod with the following characteristics was used $E= 2.1 \times 10^5 \text{N/m}^2$, $w_{MR} = 40.0 \text{ mm}$ and $d = 120.0 \text{ mm}$. F was applied through a basket containing standardized masses that were hung by a nylon thread. Static calibration was performed by means of five distinct additive masses in a vessel in the range of 0 g to 250.0 g, adding 50.0 g mass to the limit of 250.0 g. Then the masses were removed from the vessel gradually until returned to 0. Each mass measurement was repeated six times and table 1 shows loading of the masses into the vessel while table 2 shows the unloading of masses from the vessel. The least squares method was used to perform the linear regression, to obtain the linearization curve and to determine the sensitivity of E_c . The calculations involving the measurements were obtained by equation (15) and equation (16).

$$A = \frac{\sum_{i=1}^N R_i}{N} \quad (15)$$

Being A : average; R_i : measurements performed; N : number of measurements.

$$S. D = \frac{\sqrt{(R_i)^2 - A}}{N-1} \quad (16)$$

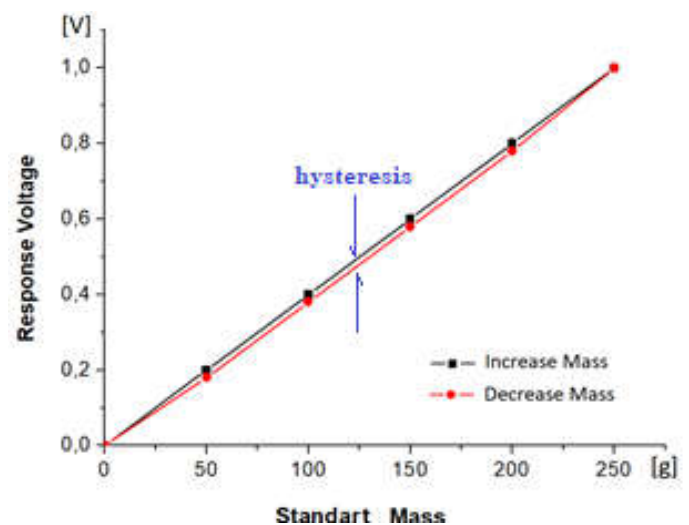
Being $S.D$: standard deviation. The hysteresis refers to the difference between two exit values for the same mass, depending on the sense (increase or decrease mass) of successive values. Equation 17 shows how to calculate the hysteresis.

$$\% \text{ hysteresis} = \frac{100MOD}{FSO} \quad (17)$$

Being MOD : maximum response difference for the same entrance and FSO : back scale output. The resolution was defined as the smallest change in the measured value at which the system is able to detect. The dynamic response of the new device was evaluated by applying force in the form of a pulse. The applied force was abruptly removed from the mass basket. The descent time is defined as the time required for the response of the extensometer to reach the value of 63% of the regime value.

RESULTS

The sensor structure was projected to operate in the elastic region. Figure 5 shows the static calibration of the new extensometer being the maximum hysteresis obtained was 3%. The MOD occurred for the force of 1.35 N. The resolution of E_c containing the signal conditioning circuit was 0.09 N, its dynamic response time when cutting the wire that contained the dish containing the standardized masses was 8.0 ms, correlation coefficient was 0.9988 and the maximum response in voltage to maximum load was 1.0 V. Figure 6 also shows another dynamic response of the E_c in a small time variation, F was applied thereto using the hand resting on S_H . Since this response is too low, it was obtained with the utilization of a digital multimeter MDM8156 of 5.5 digits. In the case of conventional E_R , it wasn't verified hysteresis, the dynamic response time was 6.0ms, correlation coefficient was 0.9999 and the maximum response in voltage for maximum load of 1.0 V of the masses was 0.20 V. Figure 7 shows the behavior of the resistive extensometer with the loading and unloading of the same standard 50 g masses, the same container and the same limits.



Source: Author

Figure 5. Static response of E_C

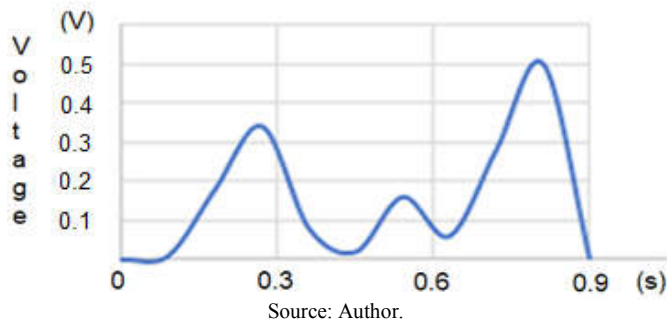


Figure 6. Dynamic response of E_C

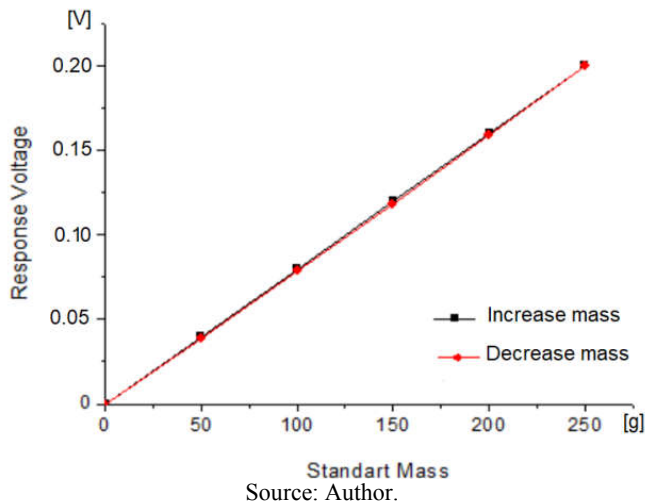


Figure 7. Response of the E_R

DISCUSSION

It is understood that the reason for the voltage response of the E_C was much greater than the response of the E_R by the fact that the first extensometer offers less opposition to the elongation or shortening of B . The verified hysteresis for the E_C is thought to be caused by the excess of inappropriate adhesive in the development of the flexible insulation film F_{IS} located between E_m . Another factor that contributes to the appearance of the hysteresis is due to the fact that E_C has not been submitted to high dynamic effort in order to increase the elasticity of the adhesive used between E_m . The response time of the 8.0 ms of E_C is worse than the response time of E_R . This fact is certainly related again to both the type and the high amount of adhesive used to attach E_m to the F_{IS} . The small standard deviation verified for both extensometers shows the stability of the same signal conditioning circuit applied for both cases. Although the constructive process of E_C can still be improved with the replacement of the adhesive, the results show the great potential of this extensometer when compared to the E_R .

The dynamic test that was performed with the right hand finger that flexed the metal rod showed that the response of the equipment depends on the speed in applying F on B .

Conclusion

The project consisted in the implementation of a capacitive extensometer that presented robustness and sensitivity when compared to the E_R . The new extensometer has higher sensitivity, 1.0 V while E_R presented 0.20 V and was also more versatile, as well as presented a virtually linear response, hysteresis of 3.0%, dynamic response time of 8.0 ms, resolution of 0.09 N and maximum standard deviation of 0.01. E_C shows a response frequently from 59 Hz. His setup at Wheatstone Bridge made his response insensitive to the temperature of the place he is exposed to. The hysteresis and response time certainly resulted from the use of the type and the amount of adhesive used in the implementation of the mobile electrodes E_m . The device can be used in the development of load cells with the objective of determining mechanical magnitudes such as force, deformation and displacement of structural systems of civil construction and Mechanical Engineering.

Acknowledgements

The National Council of Scientific and Technological Development - CNPq for the financial support in the development of this research. And finally, everyone who contributed to the accomplishment of this work, whether directly or indirectly, is registered here, thank you very much!

REFERENCES

- Areny, R. P., Webster, J. W. 1991. Sensor and Signal Conditioning. New York: Wiley.
- Cobbold, R. S. C. 1974. Transducers for Biomedical Measurements. New York: Wiley.
- Kim, S. R., Kim, J. H. Park, J. W. 2017. Wearable and Transparent Capacitive Strain Sensor With High Sensitivity Base on Patterned Ag Nanowire Networks. *Journal of ACS Appl Mater Interfaces*. 9(31): 26407-16.
- Zeiser, R., Fellner, T. Wilde, J. 2014. Capacitive strain gauges on flexible polymer substrates for wireless, intelligent systems. *Journal of Sensors and Sensor Systems – JSSS*, 3, 77–86.
- Zens, M., Niemeyer, P., Bernstein, A., Feucht, M. J., Kühle, J., Südkamp, N. P., Woias, P., Mayr, H. O. 2015. Novel approach to dynamic knee laxity measurement using capacitive strain gauges. *Journal of Knee Surg Sports Traumatol Arthrosc*. 23(10):2868-75.
